IET Generation, Transmission & Distribution

Research Article

IET Journals
The Institution of Engineering and Technology

Multi-area environmentally constrained active–reactive optimal power flow: a short-term tie line planning study

ISSN 1751-8687
Received on 22nd December 2014
Revised on 27th August 2015
Accepted on 11th October 2015
doi: 10.1049/iet-gtd.2014.1195
www.ietdl.org

Mahdi Pourakbari-Kasmaei[1] ✉, *Marcos Julio Rider*[2], *Jose Roberto Sanches Mantovani*[1]

[1]*Department of Electrical Engineering, State University of Sao Paulo, Ilha Solteira, Brazil*
[2]*Department of Systems and Energy, University of Campinas, Campinas, Sao Paulo, Brazil*
✉ *E-mail: mahdi.pourakbari@ieee.org*

Abstract: This study presents a tie line planning and its effects on the operating cost and environmental issues of power systems via a novel multi-area active–reactive optimal power flow (MA-AROPF) model. In this study, the authors focus on the significant role of tie line planning on power system operation. To select an appropriate tie line, a modified sensitivity index is used, which not only reduces the operating cost and emissions, but also enhances the voltage stability of individual areas and the entire power system. These benefits are obtained by increasing the degree of freedom of the power system through providing uniform economic and emission dispatch. Moreover, in this study, to address the drawbacks of commonly used decomposition methods for solving MA-AROPF, an integrated model is proposed. An AROPF that considers the environmental effects is a highly non-linear problem, and the multi-area consideration of such problems via tie line planning makes it an even more complicated and exceedingly non-linear problem. For didactic purposes and to verify the model, a small two-area system is considered in detail, while to show the effectiveness of the proposed approach, a three-area system consisting of 14-, 30-, and 118-bus IEEE test systems is conducted.

Nomenclature

Indices

$i,\ j,\ k$	index for the buses
ij	index for the corridor between buses i and j
l	index for the transmission lines
sa	index for the sub-areas
$x,\ y$	index for the areas

Sets

$\boldsymbol{G}(\cdot)/\boldsymbol{H}(\cdot)$	set of equality/inequality constraints of individual buses
$\boldsymbol{G}'(\cdot)/\boldsymbol{H}'(\cdot)$	set of equality/inequality constraints of interconnected buses
Ω_{A}	set of areas
$\Omega_{\mathrm{b}}^{\mathrm{A}_x}/\Omega_{\mathrm{b}}^{\mathrm{A}_{xy}}$	set of buses at area x/interconnected area xy $(x \neq y)$
$\Omega_{\mathrm{g}}^{\mathrm{A}_x}/\Omega_{\mathrm{g}}^{\mathrm{A}_x^{\mathrm{sa}}}$	set of generators at area x/area x and sub-area sa
Ω_{IA}	set of interconnected areas
$\Omega_{\mathrm{L}}^{\mathrm{A}_x}$	set of transmission lines at area x
$\Omega_{\mathrm{SA}}^{\mathrm{A}_x}$	set of sub-area at area x
$\Omega_{\mathrm{TL}}^{\mathrm{A}_{xy}}$	set of tie lines between areas x and y $(x \neq y)$

Functions

$C_i(\cdot)$	generation cost of unit i
$\overline{E}_i(\cdot)$	maximum excitation voltage of unit i
$\mathrm{Em}_i(\cdot)$	emission produced by unit i
F	objective function
$F_{\mathrm{C}}^{\mathrm{MA}}$	total cost function of a multi-area power system
$f_i^{\mathrm{A}_x}(\cdot)$	objective function of unit i at area x
$\mathrm{fl}_{ij/ji}(\cdot)$	power flow of line ij/ji
$P_{\mathrm{g}_i}^{\mathrm{M}}(\cdot)$	maximum output power of generator i, imposed by the capability curve

Variable and limits

a_{ij}^l/φ_{ij}^l	magnitude and phase of transformer tap in line l at corridor ij
$\mathrm{EMSA}_x^{\mathrm{sa}}$	emission of sub-area sa at area x
EMA_x	emission of area x
$\overline{\mathrm{EMA}_x}$	maximum emission limit of area x
EMS	system emission
$\overline{\mathrm{EMS}}$	maximum emission limit of system
$\overline{\mathrm{EMSA}}_x^{\mathrm{sa}}$	maximum emission limit of sub-area sa at area x
$\bar{f}\mathrm{l}_{ij/ji}$	maximum power flow limit of line ij/ji
$P_{\mathrm{g}_i}/Q_{\mathrm{g}_i}$	active–reactive power generation of unit i
$P_{\mathrm{d}_i}/Q_{\mathrm{d}_i}$	active–reactive power demand at bus i
$\underline{\mathrm{P}_{\mathrm{g}_i}}$	minimum active generation limit of unit i
p_{ij}/p_{ji}	direct/reverse active power flow of line ij/ji
p'_{ij}/p'_{ji}	direct/reverse active power flow of tie line ij/ji
$\underline{Q_{\mathrm{g}_i}}/\bar{Q}_{\mathrm{g}_i}$	minimum/maximum reactive generation limit of unit i
q_{ij}/q_{ji}	direct/reverse reactive power flow of line ij/ji
q'_{ij}/q'_{ji}	direct/reverse reactive power flow of tie line ij/ji
S_{g_i}	rated VA of the machine
tp_{ij}	transformer tap ratio in corridor ij
$\underline{\mathrm{tp}_{ij}}/\overline{\mathrm{tp}_{ij}}$	minimum/maximum transformer tap ratio in corridor ij
$u_i^{\mathrm{A}_x}/u_i^{\mathrm{A}_{xy}}$	control variables of bus i at area x/interconnected area xy $(x \neq y)$
$\underline{u}_i^{\mathrm{A}_x}/\bar{u}_i^{\mathrm{A}_x}$	lower/upper band of control variables of bus i at area x
$\underline{u}_i^{\mathrm{A}_{xy}}/\bar{u}_i^{\mathrm{A}_{xy}}$	lower/upper band of control variables of bus i at interconnected area xy $(x \neq y)$
v_i	voltage magnitude of bus i
$\underline{v}_i/\bar{v}_i$	maximum/minimum voltage magnitude limit of bus i
Xs_i	synchronous reactance of the machine
θ_{ij}	angle differences of a line between buses i and j

$\Psi_i^{A_x}/\Psi_i^{A_{xy}}$ state variables of bus i at area x/interconnected area xy ($x \neq y$)

π_i/κ_i Lagrange multiplier of the active–reactive demand equality constraint at bus i

Constant

$a_i,\ b_i,\ c_i$ cost coefficients of unit i

g_i^{sh}/b_i^{sh} shunt conductance/shunt susceptance of bus i

$g_{ij}^l/b_{ij}^l/b_{ij}^{l,ch}$ conductance/susceptance/charging susceptance of line l at corridor ij

n_A number of areas

$r,\ x,\ c$ resistance, reactance, and charging susceptance $b_{ij}^{l,ch}$ of line l at corridor ij

$\alpha_i,\ \beta_i,\ \gamma_i$ emission coefficients of unit i

1 Introduction

Optimal power flow (OPF) is an extension of the conventional economic dispatch and is considered as the kernel of a power system [1, 2]. A multi-area OPF, which is an adopted OPF tool for multi-area power systems, aims to determine the optimum output of all online units under steady-state conditions by optimising a predefined objective [3]. In this regard, several constraints such as active and reactive power balance, transmission and tie lines power flow limits, active and reactive power generation limits etc. are taken into account [4–6].

In addition to the importance of considering the costs, stability, and security of a power system, currently, some countries are attempting to reduce the harmful environmental impacts of generating electricity [7]. Since 1990, the Clean Air Act Amendments has mandated that utilities must modify their design or operational strategies to reduce emissions that pollute the atmosphere [8, 9]. Subsequently, two innovative approaches of cap-and-trade emission markets were introduced [10]. Power plants are moving toward using carbon capture storage technology, which is a promising option to obtain the ambitious targets of reducing carbon dioxide emissions [11]. Another method is installing desulphurisation units to reduce the harmful environmental effects of power plants [12]. Implementation of the energy-saving generation dispatching model is an innovative approach, which not only results in energy savings but also the reduction of pollutant emissions [13]. The emission limitations of a power system can be considered in the context of a system emissions limit (EMS), a regional emissions limit (EMA), and a sub-area emissions limit (EMSA), and these constraints will decrease the degrees of freedom of a power system. A system with a low degree of freedom will be faced with a serious problem of rescheduling under critical conditions such as unexpected generator outages or transmission line failures and for unanticipated spikes in the demand. Therefore, adding an appropriate tie line, by transmitting enough active and/or reactive power among the areas, is considered an applicable approach to increase the degree of freedom and to reduce the system emissions and the operating costs.

To achieve higher efficiency in a power system, the operators of small-scale systems prefer and tend to connect to other systems to form an interconnected large-scale system. Though such interconnected systems have several benefits, it is quite difficult to determine the optimal operation point of such large-scale systems, and the use of decentralised method is more practical in determining the optimal solution of such systems on an area-by-area basis [14, 15], where only a small amount of information must be interchanged among the involved areas [16]. Decomposition methods, which are the general approaches for solving the large-scale problems, through breaking it up into smaller problems via a parallel or sequential approach, try to solve such problems in DC or AC power systems [17]. To develop the algorithm for multi-area power systems, most of the relevant works have focused on DC-OPF. An iterative decentralised DC-OPF that can be implemented on a network workstation was reported in [18]. In [19], a proper and simple coordination among area operators was proposed. In [20], a non-iterative method that does not require a central coordinator was reported. In [21], a decentralised method that is based on a pricing mechanism was reported, with coordination of areas, based on the prices of the power exchange between the interconnected areas. However, the main drawback of such methodologies is their iterative manner.

In a multi-area power system, all the activities in each area will affect the prices, stability, degrees of freedom etc. of other interconnected areas. In this regard, a tie line can play an important role. From an operational standpoint of a regional transmission organisation (RTO), tie lines are used to facilitate the energy exchange between areas based on a pre-defined agreement [22]. Moreover, measuring the transmitted power between areas through a tie line requires the knowledge that whether the area is balancing its active and reactive generations and loads or not [23]. Similar to an independent system operator (ISO), the RTO coordinates, controls, and monitors the operation of a larger power system such as a multi-area power system [24]. While safety and stability are the two most important issues in an RTO, providing the security of a power system is considered as the main role of an RTO in a power system market to ensure that the supply and demand are in balance and the frequency fluctuations and interruptions, which may result in a shedding of power or a blackout, are avoided. Thus, both ISO and RTO are responsible for managing every single-area power system (appropriate generation and transmission), and also the interconnections of these areas in an online consideration via a multi-area active–reactive OPF (MA-AROPF). In this literature,

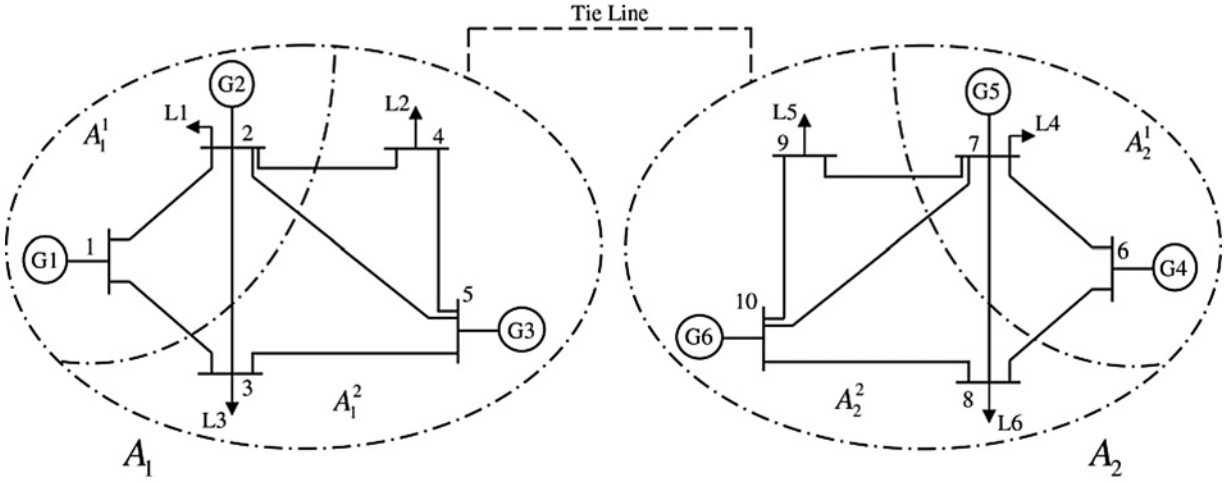

Fig. 1 *Sample two-area power system*

IET Gener. Transm. Distrib., 2016, Vol. 10, Iss. 2, pp. 299–309

two commonly used models for AROPF problem have been introduced. In [25, 26], the effects of reactive power have directly been considered on the objective function, whereas in [27, 28], the maximum active power limit is a non-linear function of reactive power, and consequently, the effects of reactive power have indirectly been considered on the objective function. The management of energy flows across the grid and the exchange of power flow information via the RTO will result in a properly functioning power system. One of the functions of the RTO is expansion planning, and more specifically, tie line planning [29]. The coordination between the generation and transmission expansion planning is a critical issue in a power system, since it can enhance the stability of each area, thereby resulting in the entire power system's stability [30]. In the multi-area power system studies, the tie lines are usually predefined and the researchers focus on decomposition approaches, security enhancement [31] etc.

Traditionally, tie line planning is performed by considering the location, the capacity of tie lines, as well as the rate of return, in order to obtain the optimal economic operation of the system. This paper focuses on the operation of a power system for which only the effects of tie lie planning are taken into consideration. To determine an appropriate tie line, three types of methods can be used: metaheuristic-, enumeration-, and sensitivity index (SI)-based methods [32]. Though metaheuristic-, and enumeration-based methods, for an economic-oriented optimisation problem, may determine the appropriate tie lines that result in a lower cost than the SI method, these methods have some drawbacks. For instance, they are time-consuming, and also inefficient in finding an appropriate tie line that satisfies several objectives. For example, in enumeration methods, it is quite difficult to find a compromise between several objectives via a classic approach, while for metaheuristics, adjusting the compromise coefficients of the objectives is a complicated task [9]. In this paper, regarding to [33], a modified SI that works based on the system voltage profile, and the Lagrange multipliers of the active and reactive demands equality constraints is proposed. The optimal tie line is considered to be the one that most effectively enhances the stability and degree of freedom of a multi-area system while reducing the total operating cost. In other words, optimal addition of tie lines result in a more stable and re-schedulable power system with a lower operating cost.

This paper aims at contributing to: (i) proposing a novel MA-AROPF model, (ii) considering the tie line planning effects on a multi-area system and demonstrating its importance, and (iii) introducing a modified SI for tie line planning problems. The proposed MA-AROPF, which is an integrated model, addresses several drawbacks of the commonly used decentralised methods and accounts for the EMS, EMA, and EMSA as the emission limits. For didactic purpose and to verify the proposed paradigm, a simple two-area test system is used, and then a large-scale three-area system containing three IEEE commonly used test cases of 14-, 30-, and 118-bus test systems is considered to show its effectiveness.

The rest of this paper is organised as follows. Section 2 contains the proposed MA-AROPF model. Case studies and results are presented in Section 3, and also an extra explanation on the tie line selection process is presented. Section 4 contains the concluding remarks and the prospects for future works.

2 Problem formulation

The main objective of an MA-AROPF problem is to minimise the entire interconnected power system's costs. Selecting proper tie lines plays a significant role to achieve this goal as well as to enhance the voltage stability of a multi-area system. It is essential to consider the environmental limits during the tie line planning process. Otherwise, the degree of freedom of the system may not be sufficient to ensure proper rescheduling when the system encounters a critical condition, and consequently, a high rescheduling cost or a failure in rescheduling may result. In this section, first, the mathematical formulation for an MA-AROPF problem is presented, followed by the presentation of the strategy of tie line planning.

2.1 MA-AROPF mathematical formulation

In this paper, to obtain the proposed multi-area model, which is fast and unequivocal, the coupling constraints are defined and the resulting formulation constitutes an MA-AROPF model. This model is readily implementable and its optimal solution can be determined by using only a commercial non-linear solver. A generalised mathematical formulation of a multi-area power system can be presented by (1)–(7)

$$\begin{aligned}\min F(\Psi,\ u) &= \sum_{x\in\Omega_{\mathrm{A}}}\Big[\min \sum_{i\in\Omega_g^{\mathrm{A}_x}} f_i^{\mathrm{A}_x}(\Psi_i^{\mathrm{A}_x},\ u_i^{\mathrm{A}_x})\Big]\\ &= \min \sum_{i\in\Omega_{\mathrm{g}}^{\mathrm{A}_1}} f_i^{\mathrm{A}_1}(\Psi_i^{\mathrm{A}_1},\ u_i^{\mathrm{A}_1})\\ &\quad + \min \sum_{i\in\Omega_{\mathrm{g}}^{\mathrm{A}_2}} f_i^{\mathrm{A}_2}(\Psi_i^{\mathrm{A}_2},\ u_i^{\mathrm{A}_2}) + \cdots\\ &\quad + \min \sum_{i\in\Omega_{\mathrm{g}}^{\mathrm{A}_{(n_{\mathrm{A}}-1)}}} f_i^{\mathrm{A}_{(n_{\mathrm{A}}-1)}}(\Psi_i^{\mathrm{A}_{(n_{\mathrm{A}}-1)}},\ u_i^{\mathrm{A}_{(n_{\mathrm{A}}-1)}})\\ &\quad + \min \sum_{i\in\Omega_{\mathrm{g}}^{\mathrm{A}_{n_{\mathrm{A}}}}} f_i^{\mathrm{A}_{n_{\mathrm{A}}}}(\Psi_i^{\mathrm{A}_{n_{\mathrm{A}}}},\ u_i^{\mathrm{A}_{n_{\mathrm{A}}}})\end{aligned} \tag{1}$$

s.t.

$$\boldsymbol{G}(\Psi_i^{\mathrm{A}_x},\ u_i^{\mathrm{A}_x}) = 0, \quad x\in\Omega_{\mathrm{A}} \tag{2}$$

$$\boldsymbol{H}(\Psi_i^{\mathrm{A}_x},\ u_i^{\mathrm{A}_x}) \le 0, \quad x\in\Omega_{\mathrm{A}} \tag{3}$$

$$\underline{u}_i^{\mathrm{A}_x} \le u_i^{\mathrm{A}_x} \le \bar{u}_i^{\mathrm{A}_x}, \quad x\in\Omega_{\mathrm{A}} \tag{4}$$

$$\overset{x\neq y}{\boldsymbol{G}'}(\Psi_i^{\mathrm{A}_{xy}},\ u_i^{\mathrm{A}_{xy}}) = 0, \quad xy\in\Omega_{\mathrm{IA}} \tag{5}$$

$$\overset{x\neq y}{\boldsymbol{H}'}(\Psi_i^{\mathrm{A}_{xy}},\ u_i^{\mathrm{A}_{xy}}) \le 0, \quad xy\in\Omega_{\mathrm{IA}} \tag{6}$$

$$\underline{u}_i^{\mathrm{A}_{xy}} \le u_i^{\mathrm{A}_{xy}} \le \bar{u}_i^{\mathrm{A}_{xy}}, \quad xy\in\Omega_{\mathrm{IA}} \tag{7}$$

where (2)–(4) are equality constraint, inequality constraint, and control variables of individual buses, respectively; and (5)–(7) are equality constraint, inequality constraint, and control variables of interconnected buses, respectively.

In this paper, the objective of all areas is to minimise the operating cost. For didactic purposes, the formulation of a tie line planning problem via MA-AROPF, for a two-area system, Fig. 1, is considered in detail

$$\begin{aligned}&\min F_{\mathrm{C}}^{\mathrm{MA}} = \min \sum_{i\in\Omega_{\mathrm{g}}^{\mathrm{A}_1}} C_i(P_{\mathrm{g}_i}) + \min \sum_{i\in\Omega_{\mathrm{g}}^{\mathrm{A}_2}} C_i(P_{\mathrm{g}_i})\\ &\text{s.t.}\quad \text{constraints sets } (9)-(17) \text{ and } (32)-(36)\end{aligned} \tag{8}$$

(see (9–17) at bottom of the next page)

where $F_{\mathrm{C}}^{\mathrm{MA}}$ is the total cost of multi-area system; and (9)–(17) are the constraints related to individual buses of each area. The cost function of unit i ($c_i(\cdot)$) is approximated by a quadratic function as described in (18)

$$C_i(P_{\mathrm{g}_i}) = a_i(P_{\mathrm{g}_i})^2 + b_iP_{\mathrm{g}_i} + c_i \tag{18}$$

Equations (9) and (10) are the active and reactive quality constraints, respectively; in these constraints the direct and reverse active and

reactive power injections are as (19)–(22)

$$p_{ij} = (a_{ij}^{l} v_i)^2 g_{ij}^{l} - (a_{ij}^{l} v_i) v_j [g_{ij}^{l} \cos(\theta_{ij} + \varphi_{ij}^{l}) + b_{ij}^{l} \sin(\theta_{ij} + \varphi_{ij}^{l})] \quad (19)$$

$$p_{ji} = g_{ij}^{l} v_j^2 - (a_{ij}^{l} v_i) v_j [g_{ij}^{l} \cos(\theta_{ij} + \varphi_{ij}^{l}) - b_{ij}^{l} \sin(\theta_{ij} + \varphi_{ij}^{l})] \quad (20)$$

$$q_{ij} = -(a_{ij}^{1} v_i)^2 \left(b_{ij}^{1} + \frac{b_{ij}^{l,\mathrm{ch}}}{2}\right) - (a_{ij}^{1} v_i) v_j \cdot [g_{ij}^{l} \sin(\theta_{ij} + \varphi_{ij}^{l}) - b_{ij}^{l} \cos(\theta_{ij} + \varphi_{ij}^{l})] \quad (21)$$

$$q_{ji} = -\left(b_{ij}^{l} + \frac{b_{ij}^{l,\mathrm{ch}}}{2}\right) v_j^2 + (a_{ij}^{l} v_i) v_j [g_{ij}^{l} \sin(\theta_{ij} + \varphi_{ij}^{l}) + b_{ij}^{l} \cos(\theta_{ij} + \varphi_{ij}^{l})] \quad (22)$$

Constraint (11) is related to the line power flow limit. This power flow can be considered as active power flow, (19) and (20), or apparent power flows as (23) and (24)

$$\mathrm{fl}_{ij} = \sqrt{p_{ij}^2 + q_{ij}^2} \quad (23)$$

$$\mathrm{fl}_{ji} = \sqrt{p_{ji}^2 + q_{ji}^2} \quad (24)$$

Constrains (12) and (13) are the active and reactive power generation limits, respectively; in (12) the upper bound is a highly non-linear function of reactive power generation. This limit is imposed by the capability curve and turbine and has three different portions as seen in (25) [34]

$$P_{\mathrm{g}_i}^{\mathrm{M}}(Q_{\mathrm{g}_i}) = \begin{cases} \left(\dfrac{P'_{\mathrm{g}_i}}{Q'_{\mathrm{g}_i} - \underline{Q_{\mathrm{g}_i}}}\right)(Q_{\mathrm{g}_i} - \underline{Q_{\mathrm{g}_i}}), & \underline{Q_{\mathrm{g}_i}} \le Q_{\mathrm{g}_i} \le Q'_{\mathrm{g}_i} \\ \sqrt{S_{\mathrm{g}_i}^2 - Q_{\mathrm{g}_i}^2}, & Q'_{\mathrm{g}_i} \le Q_{\mathrm{g}_i} \le Q''_{\mathrm{g}_i} \\ \dfrac{\sqrt{v_i^2 (\overline{E_i})^2 - (Q_{\mathrm{g}_i} X s_i + v_i^2)^2}}{X s_i}, & Q''_{\mathrm{g}_i} \le Q_{\mathrm{g}_i} \le \bar{Q}_{\mathrm{g}_i} \end{cases} \quad (25)$$

where $\bar{E}_i$ is defined as (26); the coordinates of the intersection points between the first and second portions (Q'_{g_i}, P'_{g_i}), and between second and third portions (Q''_{g_i}, P''_{g_i}), of the capability curve are calculated as (27)–(30)

$$\overline{E_i} = \sqrt{\frac{(X s_i P''_{\mathrm{g}_i})^2 + (X s_i Q''_{\mathrm{g}_i} + v_i^2)^2}{v_i^2}} \quad (26)$$

$$P'_{\mathrm{g}_i} = S_{\mathrm{g}_i} \cos(-\varphi) \quad (27)$$

$$Q'_{\mathrm{g}_i} = S_{\mathrm{g}_i} \sin(-\varphi) \quad (28)$$

$$P''_{\mathrm{g}_i} = S_{\mathrm{g}_i} \cos \varphi \quad (29)$$

$$Q''_{\mathrm{g}_i} = S_{\mathrm{g}_i} \sin \varphi \quad (30)$$

It should be noted that usually the voltage magnitude of bus i, v_i in (26), is supposed to be 1 [per unit (pu)], but in this paper, in order to have a more precise model, the actual voltage magnitude, (14), is considered.

Constraint (15) is related to the transformer tap limits; constraints (16) and (17) are the sub-area and area emission limits, respectively. In this paper, the amount of emission for each generator [$\mathrm{Em}_i(\cdot)$] is approximated by the quadratic function of (31) [35]

$$\mathrm{Em}_i(P_{\mathrm{g}_i}) = \alpha_i (P_{\mathrm{g}_i})^2 + \beta_i P_{\mathrm{g}_i} + \gamma_i \quad (31)$$

Constraints (32)–(35) are only for the buses related to interconnected areas. The advantages of this formulation are as follows: (i) no fictitious border bus is considered; therefore, a precise coordination is achieved; (ii) it is not an iterative information exchange-based methodology, and consequently, comparing with conventional decomposition approaches, it is not time-consuming and it is quite fast; (iii) it is a real-time methodology; therefore, it is appropriate for ISOs to use it in real-time electricity market; and (iv) it is capable of considering different objectives for different areas and use a proper solution methodology to solve the formed multiobjective problem such as heuristic-based or innovative methodologies [28] while in centralised model it is impossible (see (32 to 36))

To calculate the aforementioned power flows, (19)–(22) are used where in these formulation ij/ji belong to the set of tie lines between area 1 and area 2 ($ij/ji \in \Omega_{\mathrm{TL}}^{\mathrm{A}_{12}}$); constraints (34) and (35) are transformer taps and power flow limits of interconnected lines; and constraint (36) presents the total system emission limit,

$$\text{area } 1/2\,(\mathrm{A}_{1/2}) \begin{cases} P_{\mathrm{g}_i} - P_{\mathrm{d}_i} - g_i^{\mathrm{sh}} v_i^2 - \sum\limits_{\substack{ij \in \Omega_{\mathrm{L}}^{\mathrm{A}_{1/2}} \\ i \ne j}} p_{ij} - \sum\limits_{\substack{ji \in \Omega_{\mathrm{L}}^{\mathrm{A}_{1/2}} \\ i \ne j}} p_{ji} = 0, \quad i \in \Omega_{\mathrm{b}}^{\mathrm{A}_{1/2}}, \ i \notin \Omega_{\mathrm{b}}^{\mathrm{A}_{12}} \\ Q_{\mathrm{g}_i} - Q_{\mathrm{d}_i} + b_i^{\mathrm{sh}} v_i^2 - \sum\limits_{\substack{ij \in \Omega_{\mathrm{L}}^{\mathrm{A}_{1/2}} \\ i \ne j}} q_{ij} - \sum\limits_{\substack{ji \in \Omega_{\mathrm{L}}^{\mathrm{A}_{1/2}} \\ i \ne j}} q_{ji} = 0, \quad i \in \Omega_{\mathrm{b}}^{\mathrm{A}_{1/2}}, \ i \notin \Omega_{\mathrm{b}}^{\mathrm{A}_{12}} \\ \left|\mathrm{fl}_{ij/ji}(v, \theta, \mathrm{tp})\right| \le \bar{f}l_{ij/ji}, \quad \{ij/ji \in \Omega_{\mathrm{L}}^{\mathrm{A}_{1/2}} \\ \underline{P_{\mathrm{g}_i}} \le P_{\mathrm{g}_i} \le P_{\mathrm{g}_i}^{\mathrm{M}}(Q_{\mathrm{g}_i}), \quad i \in \Omega_{\mathrm{g}}^{\mathrm{A}_{1/2}} \\ \underline{Q_{\mathrm{g}_i}} \le Q_{\mathrm{g}_i} \le \bar{Q}_{\mathrm{g}_i}, \quad i \in \Omega_{\mathrm{g}}^{\mathrm{A}_{1/2}} \\ \underline{v_i} \le v_i \le \bar{v}_i, \quad i \in \Omega_{\mathrm{b}}^{\mathrm{A}_{1/2}} \\ \underline{\mathrm{tp}_{ij}} \le \mathrm{tp}_{ij} \le \overline{\mathrm{tp}_{ij}}, \quad ij \in \Omega_{\mathrm{L}}^{\mathrm{A}_{1/2}} \\ \mathrm{EMSA}_{1/2}^{\mathrm{sa}} = \sum\limits_{i \in \Omega_{\mathrm{g}}^{\mathrm{sa}_{1/2}}} \mathrm{Em}_i \le \overline{\mathrm{EMSA}_{1/2}^{\mathrm{sa}}}, \quad s \in \Omega_{\mathrm{SA}}^{\mathrm{A}_{1/2}} \\ \mathrm{EMA}_{1/2} = \sum\limits_{i \in \Omega_{\mathrm{g}}^{\mathrm{A}_{1/2}}} \mathrm{Em}_i \le \overline{\mathrm{EMA}_{1/2}} \end{cases} \quad (9) - (17)$$

Table 1 Generators data for the two-area system

Bus	a, \$/MW^2	b, \$/MW	c, \$	α, kg/MW^2	β, kg/MW	γ, kg	S_g, pu	Xs, pu	$\underline{Q_g}$, MVAr	$\overline{Q_g}$, MVAr
1, 6	0.01	40	3	0.009	−0.40	25.9	1.0	1.0	−50	15
2, 7	0.08	40	3	0.007	−0.30	28.9	1.0	1.0	−130	150
5, 10	0.05	20	5	0.007	−0.51	28.1	3.2	0.955	−140	140

defined as (37)

$$\mathrm{EMS} = \sum_{i\in\Omega_g^{A_1}} \mathrm{Em}_i + \sum_{i\in\Omega_g^{A_2}} \mathrm{Em}_i \tag{37}$$

2.2 Short-term tie line planning via an MA-AROPF

To determine an appropriate transmission tie line that results in an improvement on the system stability, decreases in the system's total operating cost, and even decreases in the regional or total system emissions, two methods, solvable via commercial solvers, can be used. The first is the enumeration-based approach that tests all of the possible tie lines between the areas. By considering a two-area system, first area with N and second area with M buses, it is necessary to solve an $N\times M$ AROPF, if only one tie line is necessary. Though the tie line planning is not a real-time problem, for large-scale multi-area power system (N and M are large), the enumeration method is a time-consuming task. Moreover, if the stability enhancement and cost minimisation take into account simultaneously, the problem becomes exceedingly complex and time-consuming. The second is an SI-based approach that works via network data and the optimal solutions of (8)–(17). In this paper, a modified Lagrange multiplier-based index (LMBI) is introduced to address the concerns about system stability, operating cost, and system's degree of freedom.

LMBI is a function of the Lagrange multipliers of equality constraints, (9) and (10), and the voltage angles of the interconnected buses, as described in (38)

$$\mathrm{LMBI}_{ij} = (\pi_i - \pi_j)(\kappa_i - \kappa_j)(\delta_i - \delta_j), \quad i \in \Omega_b^{A_1},\ j \in \Omega_b^{A_2} \tag{38}$$

A big LMBI demonstrates that one bus is under a good condition while the other is under a bad condition, and this candidate tie line can be chosen to transmit the power from a bus under proper conditions to a bus under critical conditions. The LMBIs are sorted in decreasing order to establish the priority list, the biggest is the first to be selected and the smaller is the last.

3 Case studies and results

For didactic purposes, the proposed approach is studied in detail on a two-area test system, and to demonstrate its effectiveness, a three-area power system, containing IEEE 14-, 30-, and 118-bus test cases, is conducted. The values in pu are on a 100 MVA basis. In addition, in this paper, the power factor that is used to perform the capability curve is 0.9. It should be stated that this paper is carried out only for a single time interval and the future time horizons are not considered where all the demands and limits are in hourly basis. It is worth mentioning that the renewable energy sources were not considered in this paper, since their associated uncertainties further complicate the problem. In this paper, to model the proposed approaches, a modelling language for mathematical programming is applied [36], while the non-linear problems are solved via the commercial solver KNITRO [37].

Table 2 Demand of the two-area system

Bus	Bus type	P_d, MW	Q_d, MVAr	Bus	Bus type	P_d, MW	Q_d, MVAr
1	3	0	0	6	3	0	0
2	2	65.0	24.0	7	2	52.0	22.0
3	1	165.0	11.0	8	1	39.0	10.0
4	1	90.0	24.0	9	1	70.0	23.0
5	2	0	0	10	2	0	0

Table 3 Branch data for the two-area system

Line	From	to	r, pu	x, pu	c, pu	tp
1	1	2	0.03030	0.09990	0.02540	1.000
2	1	3	0.01290	0.04240	0.01082	1.000
3	2	3	0.00176	0.00798	0.00210	0.978
4	2	4	0.00595	0.01960	0.00502	1.000
5	2	5	0.02030	0.06820	0.01738	1.000
6	3	5	0.01290	0.04240	0.01082	1.000
7	4	5	0.00176	0.00798	0.00210	1.000
8	6	7	0.03030	0.09990	0.02540	1.000
9	6	8	0.01290	0.04240	0.01082	1.000
10	7	8	0.00176	0.00798	0.00210	0.978
11	7	9	0.00595	0.01960	0.00502	1.000
12	7	10	0.02030	0.06820	0.01738	1.000
13	8	10	0.01290	0.04240	0.01082	1.000
14	9	10	0.00176	0.00798	0.00210	1.000
tie line	–	–	0.00176	0.00798	0.00210	1.000

3.1 Two-area test system

The first test system has been portrayed in Fig. 1, which contains two 5-bus systems connected via a tie line. The generators data, active and reactive demands, and the data of branches are available in Tables 1–3, respectively. Voltages are allowed to vary within the range of 0.95 and 1.05 pu, and buses are classified in three types of 1 [unregulated (load, PQ)), 2 (generator, PV), and 3 (swing). Though the diagram of this system is symmetric, in order to show the effectiveness and role of the multi-area systems, the demands

$$\text{int.area 1 and 2 } A_{12}\begin{cases} P_{g_i} - P_{d_i} - g_i^{sh} v_i^2 - \sum\limits_{\substack{ij\in\Omega_L^{A_{1/2}}\\ i\neq j}} p_{ij} - \sum\limits_{\substack{ji\in\Omega_L^{A_{1/2}}\\ i\neq j}} p_{ji} - \sum\limits_{ij\in\Omega_{TL}^{A_{12}}} p'_{ij} - \sum\limits_{ji\in\Omega_{TL}^{A_{12}}} p'_{ji} = 0, \quad i \in \Omega_b^{A_{12}} \\ Q_{g_i} - Q_{d_i} + b_i^{sh} v_i^2 - \sum\limits_{\substack{ij\in\Omega_L^{A_{1/2}}\\ i\neq j}} q_{ij} - \sum\limits_{\substack{ji\in\Omega_L^{A_{1/2}}\\ i\neq j}} q_{ji} - \sum\limits_{ij\in\Omega_{TL}^{A_{12}}} q'_{ij} - \sum\limits_{ji\in\Omega_{TL}^{A_{12}}} q'_{ji} = 0, \quad i \in \Omega_b^{A_{12}} \\ \underline{\mathrm{tp}_{ij}} \le \mathrm{tp}_{ij} \le \overline{\mathrm{tp}_{ij}}, \quad ij \in \Omega_{TL}^{A_{12}} \\ \left|\mathrm{fl}_{ij/ji}(v,\ \theta,\ \mathrm{tp})\right| \le \bar{f}l_{ij/ji}, \quad ij,\ ji \in \Omega_{TL}^{A_{12}} \\ \mathrm{EMS} \le \overline{\mathrm{EMS}} \end{cases} \tag{32)–(36}$$

Table 4 Optimal variables of two single areas

Case number and output variables		Bus 1	Bus 2	Bus 3	Bus 4	Bus 5	Bus 6	Bus 7	Bus 8	Bus 9	Bus 10	Time, s
case 1	δ, deg	0.00	−1.25	−1.44	−0.77	−0.22	0.00	0.01	−0.01	0.37	0.80	0.020
	v, pu	1.05	1.031	1.049	1.037	1.043	1.044	1.031	1.05	1.036	1.041	
	P_g, MW	88.26	14.59	0.00	0.00	219.02	0.00	0.00	0.00	0.00	161.76	
	Q_g, MVAr	−4.53	39.94	0.00	0.00	22.36	−2.69	33.30	0.00	0.00	19.27	
	P_g^M, MW	99.90	91.68	0.00	0.00	319.22	99.96	94.29	0.00	0.00	319.42	
case 2	δ, deg	0.00	−1.36	−1.63	−1.39	−1.04	0.00	0.01	−0.01	0.37	0.80	0.040
	v, pu	1.050	1.028	1.046	1.033	1.038	1.044	1.031	1.05	1.036	1.041	
	P_g, MW	**100.00**	**96.91**	0.00	0.00	124.50	0.00	0.00	0.00	0.00	161.76	
	Q_g, MVAr	0.16	24.66	0.00	0.00	31.26	−2.69	33.30	0.00	0.00	19.27	
	P_g^M, MW	**100.00**	**96.91**	0.00	0.00	318.47	99.96	94.29	0.00	0.00	319.42	
case 3	δ, deg	0.00	−1.56	−1.89	−1.61	−1.20	0.00	−0.24	−0.25	0.07	0.52	0.020
	v, pu	0.971	0.950	0.966	0.955	0.960	0.962	0.950	0.967	0.955	0.960	
	P_g, MW	99.27	**97.79**	0.00	0.00	124.50	12.19	6.24	0.00	0.00	143.24	
	Q_g, MVAr	1.98	20.91	0.00	0.00	34.86	−5.00	30.01	0.00	0.00	25.76	
	P_g^M, MW	99.98	**97.79**	0.00	0.00	318.10	99.88	95.39	0.00	0.00	318.96	

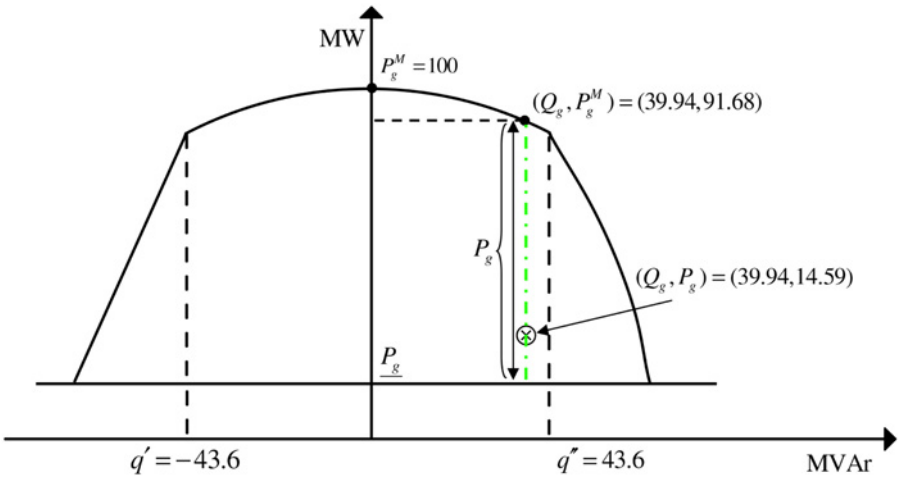

Fig. 2 *Capability curve – two single area, case 1, bus 2*

are not symmetric in such a way that the total demand of the second area is less than the first area.

Three cases are taken into consideration including the system under normal condition, system with emission limits, and system with emission limits and power flow limits.

3.1.1 Case 1: normal condition: In this case, in order to consider this two-area system under normal operating condition, no extra limitation such as emission limits or transmission line flow limit is considered.

3.1.2 Case 2: with emission limits (area, sub-area, and system emission limits): For the first area the emission limit is 285 kg, where the emission limits for its first and second sub-areas are 190 and 100 kg, respectively. For the second area, the emission limit is 255 kg, whereas the emission limit for its first and second sub-areas are 90 and 170 kg, respectively.

3.1.3 Case 3: with emission limits and line flow limit: For this case, not only the emission limits of the second case is taken into account, but also the tie line and transmission line limits have been taken into consideration. The power flow limits over transmission lines (1–2) and (7–9) are 29 and 30 MW, respectively.

To show the effectiveness of the proposed approach, at first the aforementioned three cases are analysed as single areas and afterwards the tie line planning is taken into account.

Table 4 shows the optimal values of the system variables and the total computational time [time spent in evaluation and central processing unit (CPU) time] for the three cases of two-area test system prior to tie line planning. The boldface numbers show that the generators output limit, imposed by the capability curve, has been reached. For example, this can be witnessed for bus 1 and bus 2, in case 2, and bus 2, in case 3. Operating a generator at the maximum limit adversely affects the system's degree of freedom. It is worth mentioning that the degree of freedom in the power

Table 5 Tie line ranking based on the SI (LMBI)

Case		First tie line	Second tie line	Third tie line
1	tie line	3–9	4–10	2–9
	LMBI	34.9757	30.907	25.4594
2	tie line	2–10	3–10	4–10
	LMBI	367.963	312.565	264.064
3	tie line	2–9	4–9	3–9
	LMBI	1422.89	1164.7	901.231

Table 6 System's costs ($/h) before and after adding a tie line

Case	Before tie line	After tie line		
		First	Second	Third
1	15,547.5	15,376.7	15,393.7	15,383.3
2	16,552.2	15,867.6	15,862.3	15,886.4
3	16,665.0	15,949.3	15,960.5	15,985.1

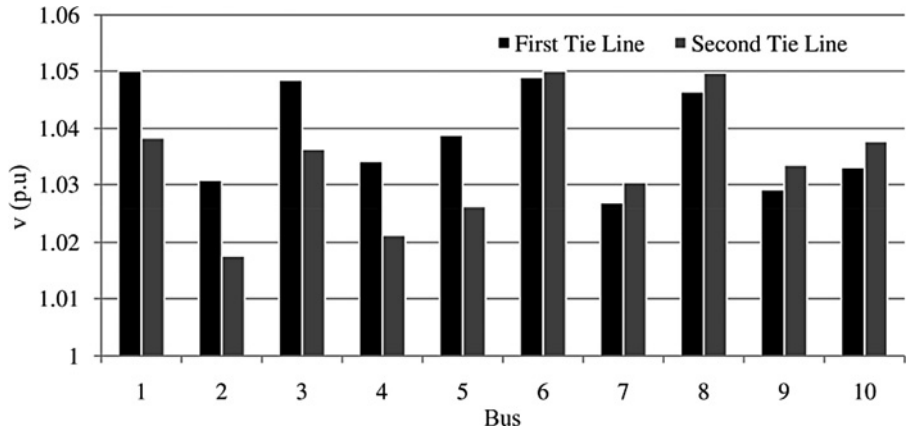

Fig. 3 *Voltage profile of the first and second tie lines – case 2, the two-area test system*

Table 7 System's emissions (kg/h) before and after adding a tie line

Case	Area	Sub-area	Before tie line	After tie line		
				First	Second	Third
1	1	1	106.02	63.87	68.89	65.98
		2	298.00	260.11	259.67	261.01
	2	1	0.00	61.05	60.44	60.53
		2	163.12	261.95	259.43	260.76
	1 and 2	1 and 2	567.14	646.98	648.43	648.48
2	1	1	179.35	112.81	107.81	121.83
		2	100.00	100.00	100.00	100.00
	2	1	0.00	88.02	90.00	79.22
		2	163.12	170.00	170.00	170.00
	1 and 2	1 and 2	442.47	470.83	467.81	471.05
3	1	1	179.45	124.51	122.80	117.29
		2	100.00	100.00	100.00	100.00
	2	1	60.34	70.49	68.63	71.51
		2	129.32	170.00	170.00	170.00
	1 and 2	1 and 2	469.11	465.00	461.43	458.80

Table 8 CSD before and after adding a tie line

Case		Before tie line	After tie line		
			First	Second	Third
1	sub-areas	124.151	114.65	112.4951	114.0765
	areas	170.342	0.72832	6.363961	4.263854
2	areas	81.30115	36.39447	36.10839	39.07898
	sub-areas	82.18702	31.24705	36.9039	18.68883
3	areas	50.16916	41.68481	42.72072	40.10466
	sub-areas	63.49112	12.0986	11.09451	19.94748

system operation is an important issue to schedule the units and to have an economic operation of the power system and an environmentally friendly scheduling.

As it is clear from Fig. 2, the maximum active generation corresponding with the $Q_g = 39.94$ MVAr is $P_g^M = 91.68$ MW and, according to (12), the active power corresponding with this reactive generation is ≤91.68 MW, the dash-dot line. Moreover, from Fig. 2 it can be seen that the optimal active power generation, $P_g = 14.59$, lies on the dash-dot line and verifies that the generator is working in its stable normal operating condition.

Table 5 presents the priority list of candidate tie lines that has been established by sorting first three biggest LMBIs in decreasing order. The reason the first three candidates are considered is to prove that the priority list is working properly, that is, the first candidate tie line has more advantages than the second, and the second candidate has more advantages than the third.

Table 6 presents the total system cost prior to and after considering the candidate tie lines. According to the results of this table, it can be concluded that by adding each single candidate tie line from the priority list, the cost has been decreased; however, the following question comes to mind: why, for example, in case 2, does the second tie line in priority list exhibit a lower cost than the first candidate? In this regard, Fig. 3 can be useful to expound. Though after adding the first tie line, the system operating cost is slightly more than adding the second one, the voltage profile of the system for these two tie lines indicates that the first tie line makes the system a more stable one. Moreover, from Table 6, it can be seen that the cases with more limitations have bigger LMBIs. This can be justified, according to the concept of Lagrange multipliers related to equality constraint, because by considering more constraints, the objective function may increase, and consequently, the Lagrange multipliers may also increase.

Table 9 Optimal variables of the two-area system – after adding the tie line

Case number and output variables		Bus 1	Bus 2	Bus 3	Bus 4	Bus 5	Bus 6	Bus 7	Bus 8	Bus 9	Bus 10	Time, s
case 1	δ, deg	0.00	−0.56	−0.63	−0.11	0.44	0.00	−0.41	−0.38	−0.31	0.33	0.047
	v, pu	1.031	1.016	1.034	1.022	1.028	1.047	1.031	1.050	1.035	1.040	
	P_g, MW	36.75	5.48	0.00	0.00	204.76	25.75	4.98	0.00	0.00	205.48	
	Q_g, MVAr	−5.65	43.52	0.00	0.00	22.50	1.48	29.69	0.00	0.00	14.96	
	P_g^M, MW	99.84	90.03	0.00	0.00	319.21	99.99	95.49	0.00	0.00	319.65	
case 2	δ, deg	0.00	−1.29	−1.57	−1.31	−0.95	0.00	−1.14	−1.08	−1.19	−0.92	0.068
	v, pu	1.050	1.032	1.050	1.036	1.040	1.050	1.028	1.048	1.031	1.035	
	P_g, MW	93.36	14.26	0.00	0.00	124.50	72.60	13.29	0.00	0.00	165.24	
	Q_g, MVAr	−10.17	38.55	0.00	0.00	19.39	5.24	34.40	0.00	0.00	18.59	
	P_g^M, MW	99.48	92.27	0.00	0.00	319.41	99.86	93.90	0.00	0.00	319.46	
case 3	δ, deg	0.00	−1.26	−1.55	−1.28	−0.91	0.00	−0.94	−0.87	−0.98	−0.42	0.059
	v, pu	1.050	1.025	1.043	1.029	1.033	1.031	1.019	1.037	1.025	1.029	
	P_g, MW	97.54	39.41	0.00	0.00	124.50	50.53	6.13	0.00	0.00	165.24	
	Q_g, MVAr	11.73	49.54	0.00	0.00	17.24	−18.60	32.02	0.00	0.00	14.84	
	P_g^M, MW	99.31	79.35	0.00	0.00	319.54	98.25	94.73	0.00	0.00	319.66	

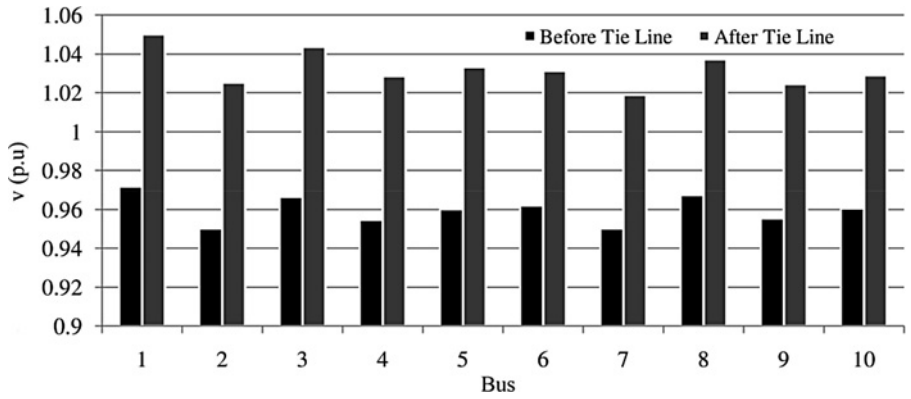

Fig. 4 *Voltage profile of the two-area system before and after adding the first tie line*

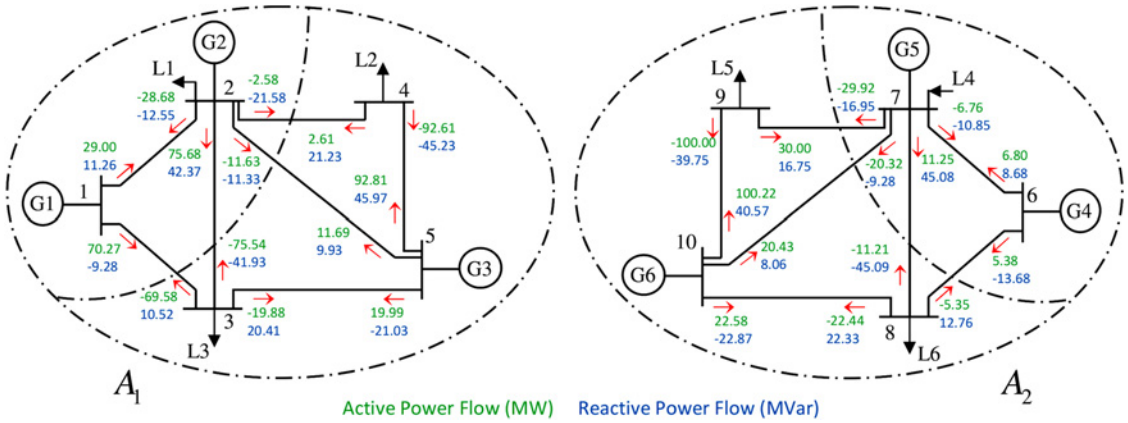

Fig. 5 *Active and reactive power flow of case 3 prior to the tie line planning*

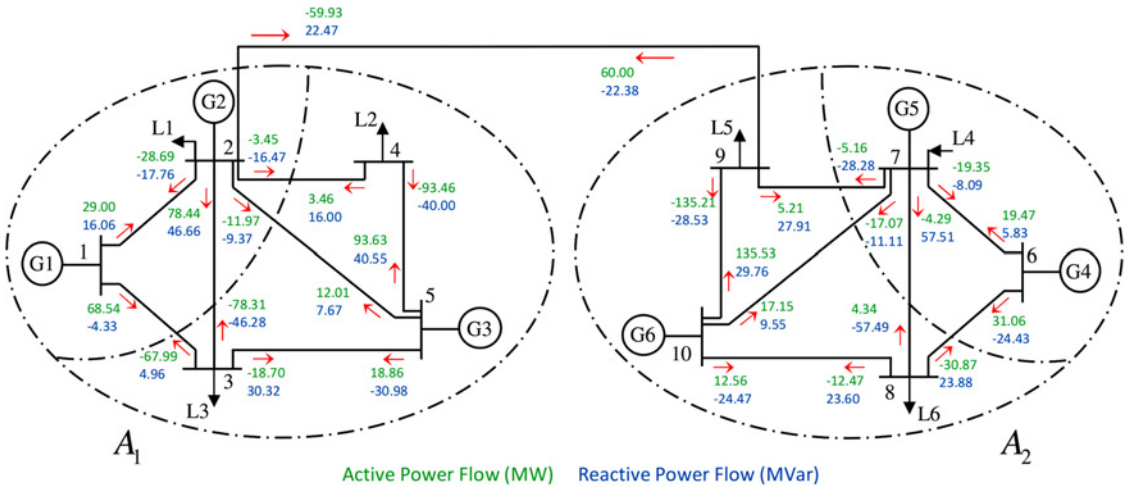

Fig. 6 *Active and reactive power flow of case 3 after adding the tie line (2–9)*

Table 7 presents the emission of each area and its sub-area and also the total emission of the two-area system prior to and after adding the tie line. As the emission function has an unexpected manner, there is not a common rule between the cost and the emission, but usually, a decrease in cost may yield an increase in emissions [38]. From this table, it is clear that for all three cases the total amount of emissions has been reduced, which means that the proposed method is a useful method in both the economic and the environmental aspects of a power system.

To demonstrate the effectiveness of tie line planning on the system emissions, which are presented in Table 7, a corrected standard deviation (CSD) is used.

The results of Table 8 indicate that, after the tie line planning, the CSDs of all three cases are less than their CDSs prior to tie line planning. However, by focusing on the areas that play a more important role than the sub-areas to exchange the power, it shows far more small CDSs than prior to the tie line planning. These results indicate that a proper tie line can result in a uniform

IET Gener. Transm. Distrib., 2016, Vol. 10, Iss. 2, pp. 299–309

Table 10 Regional (sub-area) and area emission limits (kg/h)

Area	Number of buses (numbering)	Emission limit (kg/h)			
		Area limit	Sub-area		
			Number	Number of buses	Limit
1	14 (1–14)	235	1	1 and 2	200
			2	3–14	65
2	30 (15–44)	125	1	15–21 and 27	65
			2	22–26 and 28–44	65
3	118 (45–162)	5750	1	45–67, 69–76, 157–159, and 161–162	950
			2	68, 77–117, and 160	2500
			3	118–156	2500

dispatch of emissions in the areas of the system, and consequently, a low cost, high stability, and even a low emission can then be the result. For example, as is clear from Tables 6 and 7, in case 3, adding each single tie line, not only result in a decrease in cost, but also a decrease in emissions.

Table 9 presents the optimal values of the system variables, and the total computational time (contains the time of finding the proper tie line and system operation, as well as the CPU time) after adding the first tie line (as the main tie line). The results of this table indicate that unlike the optimal values of P_g in Table 4 that have been reached their limit in some cases, after tie line planning they do not hit their limit. Therefore, the degree of freedom of the system has been enhanced, which means that when a contingency in an area occurs, more capacity is available to overcome such conditions.

Fig. 4 represents the bus voltages before and after adding the first tie line, for the case 3. It shows that prior to tie line planning the voltage profile is close to its lower limit, 0.95 pu, which may result in a voltage collapse, while after adding the first tie line, the voltage profile exhibited a significant enhancement. It proves the significant role of LMBI and the priority list in tie line planning. It exhibits significant effects not only on the voltage profile enhancement, but also on decreasing the operating cost.

To consider the case 3, which is operating under several limitations, in detail, the schematic of power flows of the two-area systems, prior to and after the tie line planning are demonstrated in Figs. 5 and 6, respectively.

As it is clear from Fig. 5, transmission lines (1–2) and (7–9) are transmitting their maximum active power flows, which yield an increase in the total operating cost, total amount of emissions, and a decrease in the degree of freedom. However, after adding the first tie line from the priority list, tie line (2–9), it can be seen from Fig. 6 that only the transmission line (1–2) has reached its limit. Therefore, it can be concluded that by adding this tie line the degree of freedom of the system has increased, and consequently, the total cost and emissions have been decreased, referring to Tables 6 and 7.

By considering the above-mentioned tables and figures for the first line as the main tie line, we can make the following conclusions. For case 1, case 2, and case 3, after adding the first tie line from the priority list, the system cost decreases by ~1.098% ($170.8), 4.14% ($684.6), and 4.29% ($715.5), respectively. However, considering the voltage profiles indicate that case 1 and case 2 are under appropriate conditions before and after adding the tie line, but for case 3, referring to Fig. 4, adding the tie line has a dramatic effect on the voltage profile.

As a conclusion of this test system, the proposed methodology for all cases has a significant effect on the reduction of the system operating cost; on the basis of the voltage profile and the generators output power as well as the uniform dispatch of emission, the stability of the system has been adjusted to a good condition, while the degrees of freedom of the system has been enhanced. Meanwhile, as is clear, the most significant effect is related to the system with the bigger LMBI, which corresponds with the critical case 3.

3.2 Three-area test system

This 162-bus multi-area system contains three different IEEE test systems including 14-, 30-, and 118-bus [39]. Area and sub-area emission limits are presented in Table 10.

For this system, first, the tie line planning without considering the tie line power flow limits is taken into account, and after adding the tie lines, the tie line power flow limit is applied. In this case study, there are three tie lines, and to find an effective tie line, three strategies can be applied.

The first strategy can be a modification of (38), as described in (39)

$$\begin{aligned}\mathrm{LMBI}_{i,j,k} = {} & (\pi_i - \pi_j)(\pi_j - \pi_k)(\pi_i - \pi_k) \\ & (\kappa_i - \kappa_j)(\kappa_j - \kappa_k)(\kappa_i - \kappa_k) \\ & (\delta_i - \delta_j)(\delta_j - \delta_k)(\delta_i - \delta_k),\ \ i \in \Omega_{\mathrm{b}}^{\mathrm{A}_1},\ j \in \Omega_{\mathrm{b}}^{\mathrm{A}_2},\ k \in \Omega_{\mathrm{b}}^{\mathrm{A}_3}\end{aligned} \tag{39}$$

The maximum amount of (39) determines the candidate tie lines. This SI will be useful to determine a connected tie line (such as a loop) for the three areas, which means that in each area, only one bus is considered as a tie line bus. The drawbacks of this formulation are as follows: (i) it cannot find a proper tie line between each of the two areas and (ii) it is not a practical strategy.

In the second strategy, after finding all of the LMBI using (38) for each of the two areas, the SI of (40) is obtained and the maximum of that index determines the candidate tie lines

$$\begin{aligned}\mathrm{LMBI}_{i,j,k} = {} & (\mathrm{LMBI}_{i,j})(\mathrm{LMBI}_{j,k}) \\ & (\mathrm{LMBI}_{i,k}),\ \ i \in \Omega_{\mathrm{b}}^{\mathrm{A}_1},\ j \in \Omega_{\mathrm{b}}^{\mathrm{A}_2},\ k \in \Omega_{\mathrm{b}}^{\mathrm{A}_3}\end{aligned} \tag{40}$$

Though using this index can compensate the main drawbacks of (39), it is not useful enough because it selects three tie lines

Table 11 Tie line sequences for the three-area system

Tie line		Set 1	Set 2	Set 3	Set 4	Set 5	Set 6
first	name	K	K	L	L	M	M
	(from, to)	(14, 15)	(14, 15)	(33, 54)	(33, 54)	(54, 14)	(54, 14)
	LMBI	49,133.2	49,133.2	49,531.8	49,531.8	7464.66	7464.66
	Cost	137,792	137,792	138,575	138,575	140,250	140,250
second	name	L	M	K	M	K	L
	(from, to)	(41, 45)	(54, 14)	(14, 42)	(50, 14)	(14, 15)	(15, 45)
	LMBI	36,602.5	59,453.2	161,300	5576.5	14,852.7	30,358.2
	cost	134,338	135,884	136,392	138,870	135,884	134,548
third	name	M	L	M	K	L	K
	(from, to)	(54, 13)	(39, 45)	(58, 14)	(13, 42)	(39, 45)	(14, 37)
	LMBI	6789.73	74,517.5	112,974	158,545	74,517.5	11,069.4
	cost	134,493	134,714	134,642	135,712	134,714	134,484

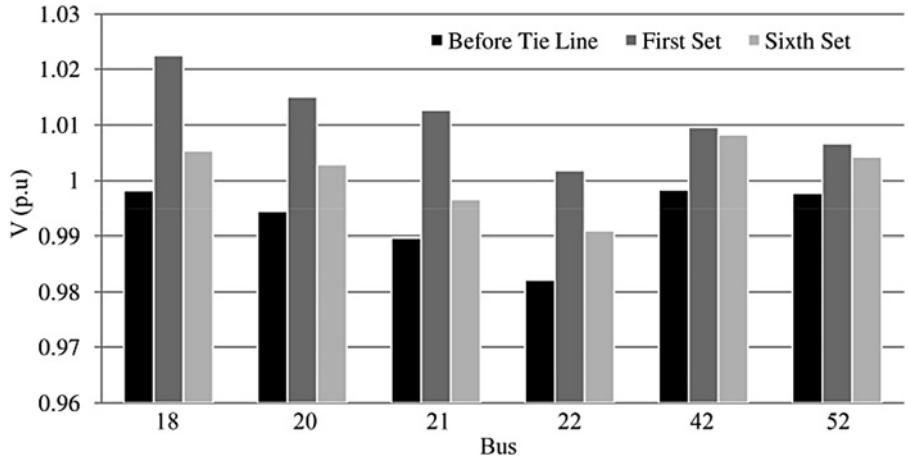

Fig. 7 *Voltage profile of the three-area system prior to and after adding the first and the sixth sets of tie lines*

Table 12 Costs ($/h) and emissions (kg/h) of the three-area system – before and after the tie line power flow limit, the first set

Area	Sub-area	Before tie line flow limit		After tie line flow limit	
		Cost, $/h	Emission, kg/h	Cost, $/h	Emission, kg/h
1	1	4170.5	100.41	3965.7	92.72
	2	1284.7	65.00	1295.1	65.00
2	1	659.8	64.75	552.6	**65.00**
	2	839.4	60.25	688.5	55.94
3	1	25,378.6	782.78	28,570.9	854.66
	2	58,302.8	2500.00	57,944.4	2500.00
	3	43,857.4	2467.22	42,478.4	2395.34
total		134,493.1	6040.41	135,495.6	6028.66

simultaneously, and adding a tie line will change the system power flow, making the two other candidate tie lines possibly not as effective as they can be after adding the first candidate tie line between the two areas.

The third strategy, which is proposed in this paper, is a sequential strategy based on (38). As in the three-area system, three tie lines are necessary, and as the sequence of connection is important, six sets (three!) must be considered. In this table, the tie lines from the first area to the second area, from the second area to the third area, and from the third area to the first area are called K, L, and M, respectively.

Table 11 presents the sequence of adding the tie lines. For example, in the first set, after determining the optimal operational point of these three areas before considering the tie lines, the total cost is $140,071 and the maximum LMBI for tie line K is 49,133.2, which is related to the candidate tie line from bus 14 to bus 15 (14, 15); after adding this candidate tie line, the cost will decrease to $137,792, and to find the next best tie line from the second area to the third area, the LMBI for the candidate lines are considered, and the maximum LMBI reveals that the tie line (41, 45) is the appropriate tie line of L; after adding L and using the new LMBI, tie line M is selected. The first set is called the KLM set. For the other possible sets (KML, LKM, LMK, MKL, and MLK), this sequential method is used to determine the tie lines.

The last row in Table 11 presents the total cost for the three-area system. To find the best set, the two items of cost and voltage profile are taken into account. First, the set that has the least cost is considered as an important candidate, and then, the voltage profile of this set is considered. The set that obtained the least cost and has an acceptable voltage profile (1 – the voltages are on the upper part of voltage interval and/or 2 – the voltages are better than or more or less the same as the system voltage profile before adding the tie lines) is selected as the best set. However, if a set is good at cost, but the voltage profile is poor, the second set with an acceptable voltage profile is selected.

Using Table 10 the best sets are the first and sixth and the first sets, which the cost of system after adding them is less than the cost obtained by adding the other sets. To select a set between the first and sixth sets, Fig. 7, which shows the voltage profile of the critical buses of the three-area test system prior to and after adding the first and sixth sets of tie lines, is considered. Since in the sixth set, there are two buses with voltages <1 pu and the average voltage profile of this set is less than the first set, the first set is selected as the most appropriate set of tie lines. After adding the tie lines of this set, the total cost will decrease to $134,493, i.e. a savings of ~3.98% in the total cost ($5578), which is a considerable savings, is obtained. Moreover, the voltage profile indicates that the minimum bus voltages for the three-area system before and after the tie line connections are 0.9822 and 1.0017 pu, which corresponds to bus 22 located in the second area; it indicates that while the maximum possible improvement for this bus is 6.903% [(1.05 – 0.9822)/0.9822], an acceptable improvement of about 1.985% [(1.0017 – 0.9822)/0.9822] has been obtained.

Table 12 presents the system's regional and total emissions and the operating costs prior to and after adding the first set of tie lines. This table indicates that, though the total system emission decreased, the regional emissions in the first sub-area of the second area (the boldface number) reached its limit, i.e. this area is working under the critical emissions condition.

4 Conclusions

In this paper, an integrated formulation for an environmentally constrained MA-AROPF was proposed, which, due to its non-iterative nature, can be a useful tool for real-time applications such as power market. In addition, for tie line planning problems modified LMBI was introduced to address the concerns about system stability, operating cost, and system's degree of freedom. By sorting the LMBIs in decreasing order, a priority list was performed. To show the usefulness of this priority list, three case studies for a small two-area test system was conducted and the results proved its significant role in tie line planning. Moreover, to show the effectiveness of the proposed model on the large-scale systems, a three-area test system was conducted. To perform the priority list, which works properly for systems with more than two areas, an efficient LMBI was introduced. Results show a considerable savings where the voltage was enhanced as well.

The results indicate that this unequivocal proposed approach not only has a great positive effect on the power system cost and emission, but also has an immense effect on the voltage stability where it will increase the degrees of freedom of the system by ensuring uniform cost and emission dispatch. Moreover, results show the rapidity of the proposed approach that makes it a useful approach for power market.

IET Gener. Transm. Distrib., 2016, Vol. 10, Iss. 2, pp. 299–309

5 Acknowledgments

This work was supported by FAPESP (nos. 2014/22828-3 and 2013/23590-8), CAPES, and CNPq (no. 305371/2012-6).

6 References

1 Zhu, J.: 'Optimization of power system operation' (John Wiley & Sons Inc., New York, NY, 2009)
2 Pourakbari-Kasmaei, M., Rider, M.J., Mantovani, J.R.S.: 'An unambiguous distance-based MIQP model to solve economic dispatch problems with disjoint operating zones', *Power Syst. IEEE Trans.*, 2015, **PP**, (99), pp. 1–2
3 Yan, Z., Xiang, N.D., Zhang, B.M., *et al.*: 'A hybrid decoupled approach to optimal power flow', *Power Syst. IEEE Trans.*, 1996, **11**, (2), pp. 947–954
4 Zhang, H., Li, P.: 'Probabilistic analysis for optimal power flow under uncertainty', *Gener. Transm. Distrib. IET*, 2010, **4**, (5), pp. 553–561
5 Zhang, H., Li, P.: 'Application of sparse-grid technique to chance constrained optimal power flow', *Gener. Transm. Distrib. IET*, 2013, **7**, (5), pp. 491–499
6 Sivasubramani, S., Swarup, K.S.: 'Sequential quadratic programming based differential evolution algorithm for optimal power flow problem', *Gener. Transm. Distrib. IET*, 2011, **5**, (11), pp. 1149–1154
7 Basu, M., Chattopadhyay, P.K., Chakrabarti, R.N., *et al.*: 'Economic emission load dispatch with non-smooth fuel cost and emission level functions through an interactive fuzzy satisfying method and evolutionary programming technique', *J. Inst. Eng. (India). Electr. Eng. Div.*, 2006, **87**, pp. 41–46
8 Lamont, J.W., Obessis, E.V.: 'Emission dispatch models and algorithms for the 1990s', *Power Syst. IEEE Trans.*, 1995, **10**, (2), pp. 941–947
9 Kasmaei, M.P., Rider, M.J., Mantovani, J.R.S.: 'A novel straightforward compromising method for dynamic economic and emission dispatch considering valve-point effect'. 2013 12th Int. Conf. on Environment and Electrical Engineering (EEEIC), 2013
10 Hobbs, B.F.: 'Emissions dispatch under the underutilization provision of the 1990 US Clean Air Act Amendments: models and analysis', *Power Syst. IEEE Trans.*, 1993, **8**, (1), pp. 177–183
11 Chen, Q., Kang, C., Xia, Q., *et al.*: 'Optimal flexible operation of a CO_2 capture power plant in a combined energy and carbon emission market', *Power Syst. IEEE Trans.*, 2012, **27**, (3), pp. 1602–1609
12 Li, L., Tan, Z., Wang, J., *et al.*: 'Energy conservation and emission reduction policies for the electric power industry in China', *Energy Policy*, 2011, **39**, (6), pp. 3669–3679
13 Ding, Y., Yang, H.: 'Promoting energy-saving and environmentally friendly generation dispatching model in China: phase development and case studies', *Energy Policy*, 2013, **57**, (0), pp. 109–118
14 Granada, M.E., Rider, M.J., Mantovani, J.R.S., *et al.*: 'Multi-areas optimal reactive power flow'. 2008 IEEE/PES Transmission and Distribution Conf. and Exposition: Latin America, 2008, pp. 1–6
15 Nogales, F., Prieto, F., Conejo, A.: 'A decomposition methodology applied to the multi-area optimal power flow problem', *Ann. Oper. Res.*, 2003, **120**, (1–4), pp. 99–116
16 Conejo, A.J., Aguado, J.A.: 'Multi-area coordinated decentralized DC optimal power flow', *Power Syst. IEEE Trans.*, 1998, **13**, (4), pp. 1272–1278
17 Boyd, S., Xiao, L., Mutapcic, A., *et al.*: 'Notes on decomposition methods'. Available at http://www.see.stanford.edu/materials/lsocoee364b/08-decomposition_notes.pdf', no date
18 Biskas, P.N., Bakirtzis, A.G., Macheras, N.I., *et al.*: 'A decentralized implementation of DC optimal power flow on a network of computers', *Power Syst. IEEE Trans.*, 2005, **20**, (1), pp. 25–33
19 Conejo, A.J., De La Torre, S., Canas, M.: 'An optimization approach to multiarea state estimation', *Power Syst. IEEE Trans.*, 2007, **22**, (1), pp. 213–221
20 Caro, E., Conejo, A.J., Minguez, R.: 'Decentralized state estimation and bad measurement identification: an efficient Lagrangian relaxation approach', *Power Syst. IEEE Trans.*, 2011, **26**, (4), pp. 2500–2508
21 Bakirtzis, A.G., Biskas, P.N.: 'A decentralized solution to the DC-OPF of interconnected power systems', *Power Syst. IEEE Trans.*, 2003, **18**, (3), pp. 1007–1013
22 Baldick, R., Chatterjee, D.: 'Coordinated dispatch of regional transmission organizations: theory and example', *Comput. Oper. Res.*, 2014, **41**, pp. 319–332
23 Alvarado, F., Oren, S.: 'Transmission system operation and interconnection', National Transmission Grid Study Issue Papers, U.S. Dept. Energy, May 2002, pp. A1–A35
24 Shahidehpour, M., Yamin, H., Li, Z.: 'Market operations in electric power systems: forecasting, scheduling, and risk management' (John Wiley & Sons Inc., New York, NY, 2002)
25 Gabash, A., Li, P.: 'Active–reactive optimal power flow in distribution networks with embedded generation and battery storage', *Power Syst. IEEE Trans.*, 2012, **27**, (4), pp. 2026–2035
26 Gabash, A., Li, P.: 'Flexible optimal operation of battery storage systems for energy supply networks', *Power Syst. IEEE Trans.*, 2013, **28**, (3), pp. 2788–2797
27 Almeida, K.C., Senna, F.S.: 'Optimal active–reactive power dispatch under competition via bilevel programming', *Power Syst. IEEE Trans.*, 2011, **26**, (4), pp. 2345–2354
28 Pourakbari-Kasmaei, M., Rider, M.J., Mantovani, J.R.S.: 'An unequivocal normalization-based paradigm to solve dynamic economic and emission active–reactive OPF (optimal power flow)', *Energy*, 2014, **73**, pp. 554–566
29 'Regional transmission organizations'. Available at http://www.ferc.gov/legal/maj-ord-reg/land-docs/2000A.pdf'Fed. Energy Regul. Comm., no date
30 Khodaei, A., Shahidehpour, M., Wu, L., *et al.*: 'Coordination of short-term operation constraints in multi-area expansion planning', *Power Syst. IEEE Trans.*, 2012, **27**, (4), pp. 2242–2250
31 Liu, C., Wang, J., Fu, Y., *et al.*: 'Multi-area optimal power flow with changeable transmission topology', *Gener. Transm. Distrib. IET*, 2014, **8**, (6), pp. 1082–1089
32 Rahmani, M., Romero, R., Rider, M.J.: 'Strategies to reduce the number of variables and the combinatorial search space of the multistage transmission expansion planning problem', *IEEE Trans. Power Syst.*, 2013, **28**, (3), pp. 2164–2173
33 Da Silva, E.L., Ortiz, J.M.A., de Oliveira, G.C., *et al.*: 'Transmission network expansion planning under a Tabu Search approach', *Power Syst. IEEE Trans.*, 2001, **16**, (1), pp. 62–68
34 Rueda, S.M.V., Almeida, K.C.: 'Optimal power flow solutions under variable load conditions: reactive power cost modeling'. 22nd IEEE Power Engineering Society Int. Conf. on Power Industry Computer Applications, 2001. PICA 2001. Innovative Computing for Power – Electric Energy Meets the Market, 2001, pp. 300–305
35 Venkatesh, P., Gnanadass, R., Padhy, N.P.: 'Comparison and application of evolutionary programming techniques to combined economic emission dispatch with line flow constraints', *Power Syst. IEEE Trans.*, 2003, **18**, (2), pp. 688–697
36 Fourer, R., Gay, D.M., Kernighan, B.W.: 'AMPL: a modeling language for mathematical programming' (Duxbury Press, 2002)
37 Byrd, R., Nocedal, J., Waltz, R.: 'KNITRO: an integrated package for nonlinear optimization', in Di Pillo, G., Roma, M. (EDs.): 'Large-scale nonlinear optimization' (Springer, US, 2006), pp. 35–59
38 Pourakbari-Kasmaei, M., Rider, M.J., Mantovani, J.R.S.: 'Congestion effect on consumers allocated cost and system emission via environmental active–reactive OPF'. Third Int. Conf. on Electric Power and Energy Conversion Systems (EPECS'13), 2013
39 Online: 'System data'. Available at www.mahdipk.com/data.html